Dynamic Numerical Analysis of Antimoisture-Damage Mechanism of Permeable Pavement Base

Xin-zhuang Cui[1]

Abstract: As a permeable base material of pavement, the large stone porous asphalt mixture (LSPM) is used widely in China to lessen the moisture damage of the asphalt pavement. However, the dynamics mechanism of the inhibitory effect of permeable base on moisture damage is not clear yet. The dynamic fluid-solid coupling analysis of the saturated pavement with LSPM base course, considering the asphalt mixtures as the porous medium, was performed using the finite difference numerical code FLAC3D. Numerical results revealed that the positive and negative dynamic pore pressure alternated in the pavement with the approaching and leaving of the wheel loads. The phenomenon of water pumping out of and sucking into the pavement under the moving loads was proved. The flow of fluid in pavement can be regarded as the laminar flow. The presence of the LSPM base course greatly decreased the dynamic pore pressure and the scouring force in the surface course because of the large permeability coefficient of the LSPM. The location of the maximum dynamic pore pressure also changed due to the LSPM base course. Due to the permeable base, the dissipation of the dynamic pore pressure was accelerated and thus the moisture damage was lessened.

DOI: 10.1061/(ASCE)GM.1943-5622.0000030

CE Database subject headings: Asphalt pavements; Moisture; Pore pressure; Numerical analysis; China; Damage.

Author keywords: LSPM pavement; Moisture damage; Dynamic pore pressure; Moving wheel load.

Introduction

One of the major factors that cause frequent pavement maintenance is moisture damage. Moisture damage can destroy the cohesive bond within the asphalt binder or the adhesive bond between the aggregate and the binder. As a result, distresses such as stripping, pot holes, pumping, and cracking occur in the asphalt pavement, and consequently the inner structure is seriously damaged (Chen et al. 2004; Kandhal 1994; Masad et al. 2004; Mallick et al. 2005).

Moisture damage includes two damage-inducing processes: physical and mechanical (Kringos and Scarpas 2008). The physical process refers to the emulsification and replacement of the asphalt membrane by moisture. Even without any mechanical loading, moisture has a degrading effect on the material properties. This implies that moisture makes a physical change to the material properties. The mechanical process refers to the acceleration process of the pavement failure under the coupling action of the vehicle load and the moisture. When the pavement is saturated or nearly saturated, under the moving wheel loads, the positive and then the negative pore pressures are generated, and synchronously the process where water is pumped out of and then sucked into the asphalt pavement surface course occurs. Under the scouring force of high pressure water, asphalt membrane is stripped from aggregate surface. This is the accepted dynamics mechanism of moisture damage. Dynamic pore pressure plays an important role during moisture damage process. However, the data in situ of dynamic water pressure are scarce. Although Liu et al. (2002) attempted to measure it, the peak value of dynamic pore pressure and the process of development and dissipation were not obtained because the sampling frequency was too low. Al-Omari and Masad (2004) and Muhammed (2005) used X-ray CT technique to obtain the three-dimensional (3D) real pore structures of asphalt concrete specimen, and then simulated the numerous steady and unsteady fluid flows. Kettil et al. (2005) used FEM to simulate the dynamic pore pressure in pavement structure, however, 3D computation was found to be unstable.

In China, the semirigid pavement is very popular. For the semirigid pavement, however, reflective cracking and moisture damage occur frequently. In order to prevent reflective cracking and moisture damage, the large stone porous asphalt mixture (LSPM) is used widely as the base course material in China, especially in Shandong province. As a permeable asphalt mixture, LSPM has the largest nominal diameter greater than 26.5 mm and the large porosity to discharge water freely from pavement structure. With respect to the antimoisture-damage effect of LSPM base course (LSPMBC), the draining effect of LSPMBC is obvious; however, the inhibitory effect on the wheel load-induced dynamic pore pressure is not clear and no work was found in literatures.

In this paper, the dynamic fluid-solid coupling analysis of a typical LSPM pavement was performed using commercially available finite difference numerical code FLAC3D. To demonstrate the antimoisture-damage effect of permeable base, the pavement without the LSPMBC was also analyzed. The numerical results were compared with those of other researchers and the field test results.

[1]Associate Professor, Dept. of Transportation Engineering, School of Civil Engineering, Shandong Univ., Jingshi Rd. 17923, Jinan, Shandong 250061, People's Republic of China. E-mail: cuixz@sdu.edu.cn

Note. This manuscript was submitted on August 8, 2009; approved on April 5, 2010; published online on April 10, 2010. Discussion period open until May 1, 2011; separate discussions must be submitted for individual papers. This paper is part of the ***International Journal of Geomechanics***, Vol. 10, No. 6, December 1, 2010. ©ASCE, ISSN 1532-3641/2010/6-230–235/$25.00.

Downloaded 02 Apr 2011 to 159.226.230.152. Redistribution subject to ASCE license or copyright. Visit http://www.ascelibrary.org

Table 1. Input Parameters for Analysis of Pavement with LSPMBC

Course name	Material name	T (cm)	E (MPa)	c (kPa)	ϕ (degrees)	k (10^{-8} m/s)
Upper surface course (USC)	AK-16A asphalt concrete	4	1,148	—	—	213
Middle surface course (MSC)	AC-25I asphalt concrete	6	984	—	—	107
Lower surface course (LSC)		8	820	—	—	
LSPM base course (LSPMBC)	LSPM	12	500	—	—	3,000
Base course (BC)	Cement-stabilized macadam	32	1,500	—	—	—
Subbase course (SBC)	Flyash-lime soil	18	750	—	—	—
Road bed (RB)	Silty clay	80	42.0	32	20	—
Upper embankment (UE)		70	41.4	26	16	—
Lower embankment (LE)		100	41.0	23	14	—

Dynamic Fluid-Solid Coupling Theory

In general, when the porosity of asphalt mixture ranges from 8 to 15%, the moisture damage is most serious because water easily flows to the pavement surface course and is difficult to be drained out. In this case, asphalt mixture can be considered as a porous medium. According to the Biot consolidation theory, the dynamic equilibrium equation of 3D saturated elastic porous medium is

$$G\nabla^2 \boldsymbol{u} + \frac{G}{1-2v}\nabla \ \text{div}\ \boldsymbol{u} = \nabla p_p + (1-n)\rho_s \frac{\partial \boldsymbol{v}_s}{\partial t} + n\rho_f \frac{\partial \boldsymbol{v}_f}{\partial t} \quad (1)$$

where $\boldsymbol{u}$ and $\boldsymbol{v}_s$=displacement vector and the velocity vector of solid medium, respectively; $\boldsymbol{v}_f$=velocity vector of fluid; G, v, n and ρ_s=shear modulus, the Poisson's ratio, the porosity and the density of solid medium, respectively; ρ_f=density of fluid; and p_p=pore pressure.

The continuous seepage differential equation is

$$\frac{k}{\gamma_f}\nabla^2 p_p = n\beta_f \frac{\partial p}{\partial t} + \frac{\partial(\text{div}\ \boldsymbol{u})}{\partial t} \quad (2)$$

where k=coefficient of permeability; β_f=compression coefficient of fluid; and γ_f=bulk density of fluid.

The flow of fluid causes the scouring force on solid skeleton, which is called seepage force in continuous porous medium mechanics. Seepage force is a kind of bulk force and can be expressed as

$$j = \gamma_f i \quad (3)$$

where i=hydraulic gradient that is the water head loss per unit seepage length.

Material Models and Mechanics Parameters

Two pavements were analyzed—one with LSPMBC and one without LSPMBC. The pavement structure with the LSPMBC is shown in Table 1. The one without the LSPMBC has the same pavement materials and dimensions except the LSPMBC.

The elastic constitutive model was used to describe the materials of the surface course, the base course and the subbase course. The Mohr-Coulomb elastic-plasticity model was employed to describe the embankment soil. The material name, the course thickness T, the Young's modulus E, the permeability coefficient k, and the cohesion c and the internal friction angle ϕ of soil of each course of pavement are shown in Table 1. During the analyses, the surface course and the LSPMBC were considered as porous and saturated medium. The porosities of the surface course asphalt mixture and the LSPM are 8 and 18%, respectively. The cement-stabilized macadam base course is assumed impermeable. All the input parameters for numerical analysis were from laboratory tests.

In analysis, the dampening was calculated with the Rayleigh linear combination method

$$\boldsymbol{C} = \alpha \boldsymbol{M} + \beta \boldsymbol{K} \quad (4)$$

where $\boldsymbol{C}$, $\boldsymbol{M}$, and $\boldsymbol{K}$=dampening matrix, mass matrix, and stiffness matrix, respectively, and α and β=constants related to the natural frequency ω and the damping ratio ξ of the pavement structure, $\alpha=\xi\omega$, $\beta=\xi/\omega$. According to model analysis, ω is 12 Hz. ξ was taken as 0.01.

Simulation of Moving Wheel Load and Boundary Conditions

The finite difference program FLAC3D (3D Fast Lagrangian Analysis of Continua) provided by Itasca Consulting Group was employed to execute the coupled analysis of saturated asphalt pavement under moving loads. The multiphysical field coupled analysis function of FLAC3D is powerful, and has been widely used widely in civil engineering.

Fig. 1 shows the geometric model, which is 28 m in the longitudinal direction (the moving direction of wheel) and 36 m in the transversal direction. Because the distance of the geometric model center point $\boldsymbol{o}$ from the boundaries is large enough, the center point $\boldsymbol{o}$ can represent very accurately any point on the real pavement surface. The wheel load was simplified as a moving

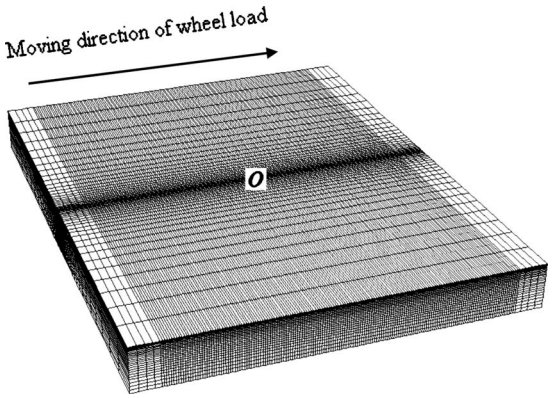

Fig. 1. Geometric model

Downloaded 02 Apr 2011 to 159.226.230.152. Redistribution subject to ASCE license or copyright. Visit http://www.ascelibrary.org

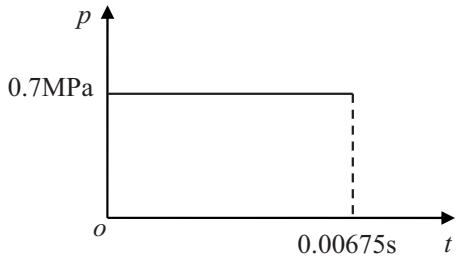

Fig. 2. Wheel load model

uniform pressure circle with the diameter of 0.3 m. As shown in Fig. 2, the tire pressure is 0.7 MPa and constant with time. The pressure circle skipped ahead 0.15 m every 0.006 75 s to simulate moving wheels with the speed of 80 km/h. The variation curve of the distance of the load circle center from the geometric model center point ***o*** versus time is shown in Fig. 3.

In the numerical dynamic calculation, the main error is from the treatment that the infinity region is replaced with the finite region. Setting manual boundary is an effective method to decrease this error. The viscous boundary method introduced by Lysmer and Kuhlemeyer (1969) was employed on infinite boundaries to absorb energy of the stress wave and prevent the stress wave from reflecting.

The cement-stabilized macadam base course is impervious, so on its surface the hydraulic gradient along the vertical direction is zero

$$\partial p_p/\partial z = 0 \tag{5}$$

where p_p=pore pressure. On road face, p_p is zero.

Numerical Results and Analyses

For the skip loading mode of wheel pressure circle, the response curves of pavement obtained from the numerical analysis need to be smoothed. Since the skip frequency is 148.15 Hz, the waves with frequencies more than 148 Hz were filtered. As a demonstration, Fig. 4 shows the original and smoothed time history curves of dynamic pore pressure at the top of the LSPMBC under the center point ***o***.

Dynamic Deflection

Defining that the upward dynamic deflection of the pavement under the moving load is positive, the time history curves of the deflection at the center point ***o*** are shown in Fig. 5. It can be seen

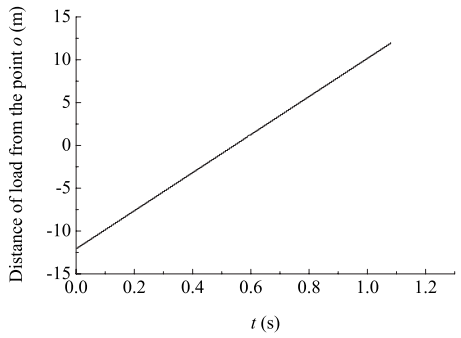

Fig. 3. Moving curve of wheel load

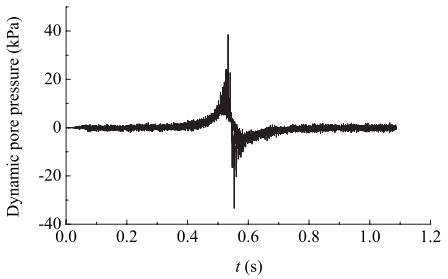

(a) Original

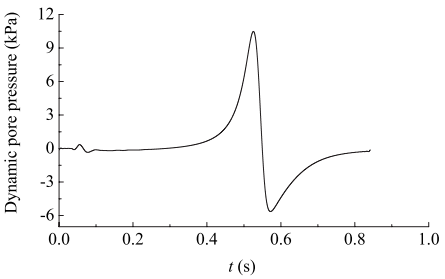

(b) Smoothed

Fig. 4. Smoothing of original dynamic pore pressure curve

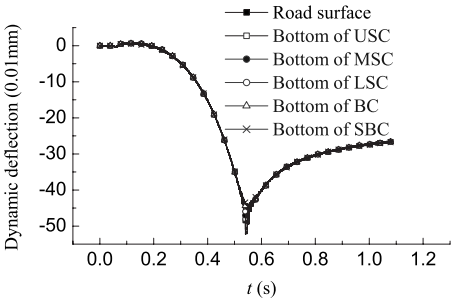

(a) Without LSPM base course

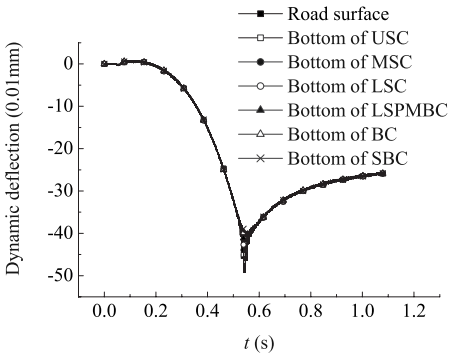

(b) With LSPM base course

Fig. 5. Time history curves of road surface deflection

Downloaded 02 Apr 2011 to 159.226.230.152. Redistribution subject to ASCE license or copyright. Visit http://www.ascelibrary.org

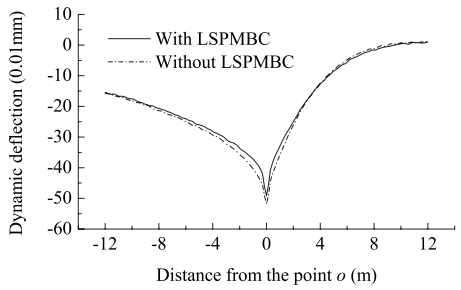

Fig. 6. Curves of deflection distribution in the longitudinal direction

that the development of the dynamic deflection is faster than its disappearance due to the dynamic effect of the moving load. This causes the asymmetry of the deflection basin on road surface in the longitudinal direction, as shown in Fig. 6. The effect of the LSPMBC on the deflection is little.

Dynamic Pore Pressure

Fig. 7 shows the development and dissipation curves of dynamic pore pressure under the center point ***o***. With the moving load approaching and leaving the center point ***o***, the dynamic pore pressure goes through two stages: the positive stage and the negative stage. The negative pore pressure is also called the suction. The result proves the process that water is pumped out of and sucked into pavement repetitively under traffic loads.

The presence of the LSPMBC greatly affects the dynamic pore pressure. Fig. 8 shows the vertical distribution of the dynamic pore pressure peak value. For the pavement without the LSP-

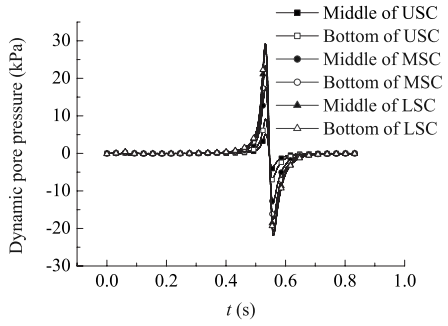

(a) Without LSPM base course

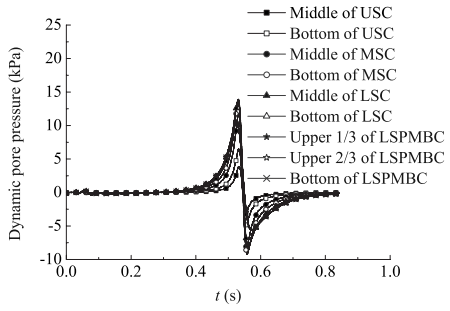

(b) With LSPM base course

Fig. 7. Time history curves of dynamic pore pressure

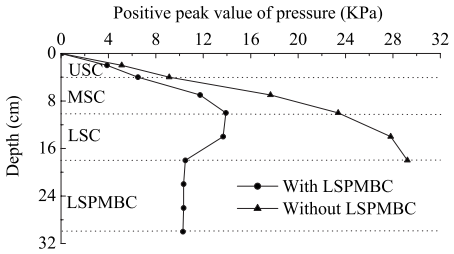

(a) Positive peak value

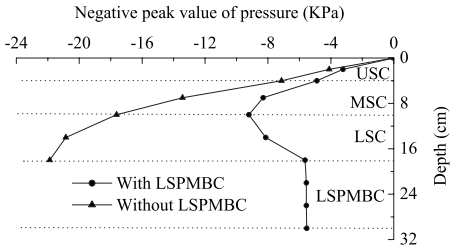

(b) Negative peak value

Fig. 8. Vertical distribution of dynamic pore pressure peak value

MBC, the maximum absolute peak values of the dynamic pore pressure all appear at the bottom of the lower surface course. However, for the pavement with the LSPMBC, the maximum peak values decrease greatly and appear at the bottom of the middle surface course. This is because the permeability coefficient of LSPM is large and improves the drainability of pavement.

Kettil et al. (2005) used the two-dimensional (2D) finite-element model to calculate the dynamic pore pressure. Compared with the 2D results, the dynamic pore pressure shown in Fig. 7(a) is low. This is mainly because the pavement is impervious in the traffic direction for the 2D model.

In order to verify the numerical result of the dynamic pore pressure, a field test was carried out. The schematic plot of the testing vehicle and its axle distances and axle loads are shown in Fig. 9. The structure of the test pavement is similar with the one listed in Table 1. Fig. 10 shows the variation curve of dynamic pore pressure in the middle of the middle surface course. Comparing Fig. 8 with Fig. 10, the absolute values of the maximum and minimum dynamic pore pressures in the middle of the middle surface course from the numerical analysis are a little less than the test results. This may be because only one wheel load was considered as the moving load in the numerical calculation and the superposition effect of loads was ignored.

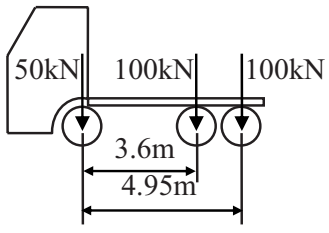

Fig. 9. Schematic plot of testing vehicle

Downloaded 02 Apr 2011 to 159.226.230.152. Redistribution subject to ASCE license or copyright. Visit http://www.ascelibrary.org

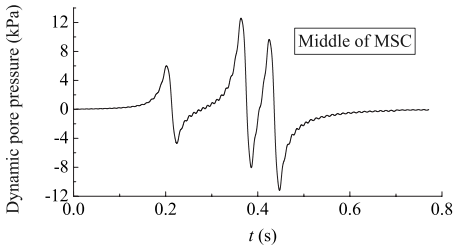

Fig. 10. Test curves of dynamic pore pressure versus time

Dynamic Stress

According to Terzaghi's effective stress principle of the porous medium mechanics, the total normal stress includes two parts: the effective stress and the pore pressure. Curves of the vertical total normal stress, the effective stress and the dynamic pore pressure versus time are shown in Fig. 11. The dynamic pore pressure changes the stress wave shape. However, the effective stress amplitude is almost the same with the total stress.

Defining the moving direction of the wheel load as the longitudinal direction, Fig. 12 shows time history curves of the longitudinal normal stress. It can be seen that the longitudinal normal stress is tensile stress and the stress amplitude is not related with the LSPMBC on the whole. This implies that the LSPMBC cannot prevent the initiation of the microcrack in subbase course. However, according to the fracture mechanics, the LSPMBC can prevent the reflective cracking from extending into the surface course due to its large porosity.

Dynamic Seepage Force

Time history curves of dynamic seepage force on asphalt mixture are shown in Fig. 13. Note that the upward seepage force is positive. As dynamic pore pressure, the positive and negative seepage

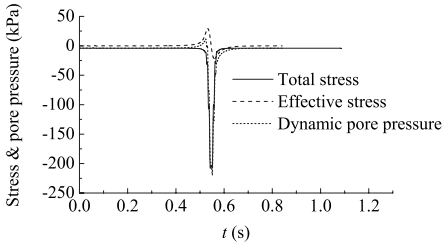

(a) Without LSPM base course

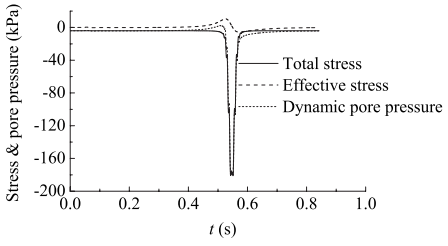

(b) With LSPM base course

Fig. 11. Time history curves of total and effective stress and dynamic pore pressure

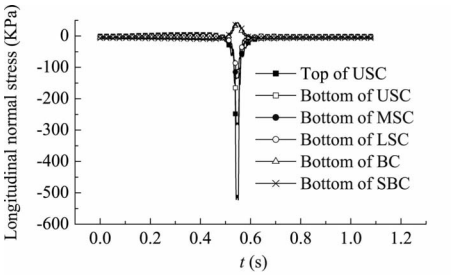

(a) Without LSPM base course

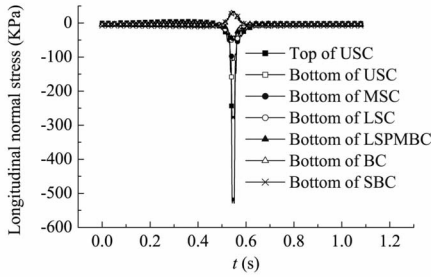

(b) With LSPM base course

Fig. 12. Time history curves of longitudinal normal stress

forces are also alternant. The presence of the LSPMBC greatly affects the seepage force. For the pavement without the LSPMBC, the maximum absolute peak values of the seepage force appear at the top of the middle surface course. For the pavement with the LSPMBC, however, the maximum peak values decrease greatly and appear at the top of upper surface course. Fig. 14 shows time history curves of longitudinal seepage force at the

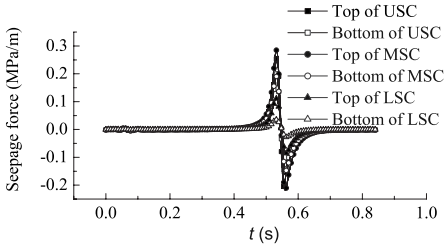

(a) Without LSPM base course

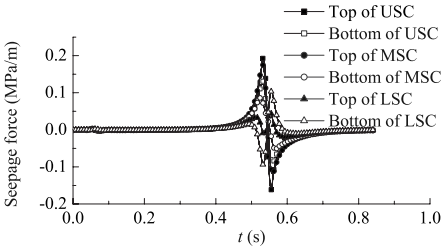

(b) With LSPM base course

Fig. 13. Time history curves of seepage force

Downloaded 02 Apr 2011 to 159.226.230.152. Redistribution subject to ASCE license or copyright. Visit http://www.ascelibrary.org

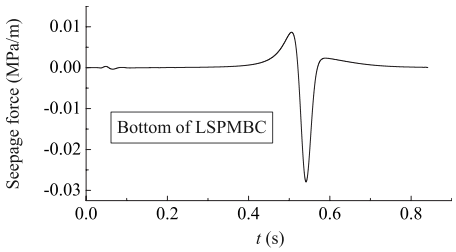

Fig. 14. Longitudinal seepage force curves at the bottom of the LSPMBC

bottom of the LSPMBC. The seepage force in the LSPMBC is much less than in the surface course; therefore, the fluid flows out of the pavement more easily and the dynamic pore pressure dissipates mainly through the LSPMBC

Under the high pore pressure and large scouring force, the emulsification and replacement of the asphalt membrane by water are accelerated. Asphalt membrane is damaged and scoured out of pavement surface gradually and finally, the aggregates without cohesion are taken away by high speed wheels. This is the whole process of moisture damage.

Dynamic Flow of Fluid

Fig. 15 shows the vertical flow velocity of fluid at the top of the upper surface course. The velocity is very small and the corresponding Reynolds number is also very small. This implies that the flow of fluid in the surface course is laminar flow. Fig. 15 gave very similar results with FEM calculation (Kettil et al. 2005).

Fig. 16 shows the longitudinal flow velocity of fluid at the bottom of the LSPMBC. The flow velocity in the LSPMBC is one order of magnitude more than in the surface course. The faster dynamic flow of fluid in the LSPMBC reduces the dynamic pore pressure in surface course and lessens the moisture damage.

Conclusions

The fluid-solid coupling analysis of the saturated pavement with the LSPMBC was carried out based on FLAC3D to explain the inhibitory effect of permeable base on moisture damage. The following main conclusions were drawn:

1. Positive and negative dynamic pore pressure alternated in the pavement with the approaching and leaving of the wheel loads.

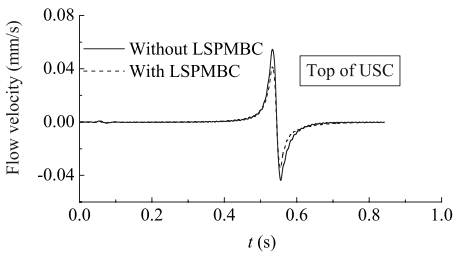

Fig. 15. Vertical flow velocity of fluid at the top of the upper surface course

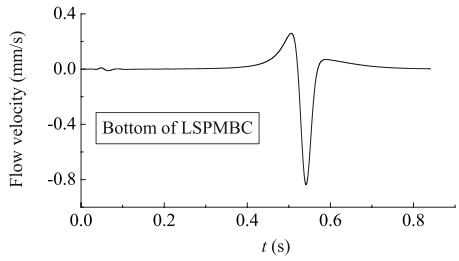

Fig. 16. Longitudinal flow velocity of fluid at the bottom of the LSPMBC

2. Dynamic flow velocity of fluid is very small and the dynamic flow in asphalt pavement is laminar flow. The dynamic flow in the LSPMBC is much faster than in the surface course.
3. Because of the large permeability coefficient, the LSPM greatly reduces the dynamic pore pressure and the scouring force in the surface course.
4. LSPMBC improves the dynamic drainability of pavement. This is the dynamic mechanism of the antimoisture damage.

Acknowledgments

This work was supported by the Chinese Natural Science Foundations (Grant Nos. 50708056 and 51078222), Shandong Province Reward Fund for Excellent Young and Middle-aged Scientists (Grant No. 2008BS09015), and Key Technologies R&D Program of Shandong Province (Grant No. 2008GG10006009).

References

Al-Omari, A., and Masad, E. (2004). "Three-dimensional simulation of fluid flow in X-ray CT images of porous media." *Int. J. Numer. Analyt. Meth. Geomech.*, 28(13), 1327–1360.

Chen, J. S., Lin, K. Y., and Young, S. Y. (2004). "Effects of crack width and permeability on moisture-induced damage of pavements." *J. Mater. Civ. Eng.*, 16(3), 276–281.

Kandhal, P. S. (1994). "Field and laboratory investigation of stripping in asphalt pavements: State of the art report." *Transp. Res. Rec.*, 80(1454), 36–47.

Kettil, P., Engström, G., and Wiberg, N. E. (2005). "Coupled hydro-mechanical wave propagation in road structures." *Comput. Struct.*, 83(21-22), 1719–1729.

Kringos, N., and Scarpas, A. (2008). "Physical and mechanical moisture susceptibility of asphaltic mixtures." *Int. J. Solids Struct.*, 45, 2671–2685.

Liu, P., Ling, H. W., and Han, J. (2002). "Measurement of pore water pressure in asphalt pavement." *Shanghai Highway*, 10(4), 20–22.

Lysmer, J., and Kuhlemeyer, R. L. (1969). "Finite dynamic model for infinite media." *J. Eng. Mech.*, 95(2), 859–877.

Mallick, R. B., Pelland, R., and Hugo, F. (2005). "Use of accelerated loading equipment for determination of long term moisture susceptibility of hot mix asphalt." *Int. J. Pavement Eng.*, 6(2), 125–136.

Masad, E., Birgisson, B., Al-Omari, A., and Cooley, A. (2004). "Analytical derivation of permeability and numerical simulation of fluid flow in hot-mix asphalt." *J. Mater. Civ. Eng.*, 16(5), 487–496.

Muhammed, E. K. (2005). "Modeling moisture transportation in asphalt pavements." Ph.D. thesis, Univ. of Maryland, College Park, Md.

Downloaded 02 Apr 2011 to 159.226.230.152. Redistribution subject to ASCE license or copyright. Visit http://www.ascelibrary.org